Nanotechnology **24** (2013) 455703 (5pp) doi:10.1088/0957-4484/24/45/455703

Strain effects in a single ZnO microwire with wavy configurations

Jong Bae Park[1,2], Woong-Ki Hong[1], Tae Sung Bae[1], Jung Inn Sohn[2], SeungNam Cha[2], Jong Min Kim[2], Jongwon Yoon[3] and Takhee Lee[4]

[1] Jeonju Center, Korea Basic Science Institute, Jeonju, Jeollabuk-do 561-180, Korea
[2] Department of Engineering Science, University of Oxford, Oxford OX1 3PJ, UK
[3] School of Materials Science and Engineering, Gwangju Institute of Science and Technology, Gwangju 500-712, Korea
[4] Department of Physics and Astronomy, Seoul National University, Seoul 151-747, Korea

E-mail: wkh27@kbsi.re.kr

Received 11 April 2013, in final form 30 August 2013
Published 18 October 2013
Online at stacks.iop.org/Nano/24/455703

Abstract
We investigate strain-induced optical modulation in a ZnO microwire with wavy geometries induced by mechanical strains. Curved sections of the wavy ZnO microwire show red-/blue-shifts of near-band-edge emission and broadening of full width at half maximum in cathodoluminescence spectra along the length of the wavy ZnO microwire, compared with straight sections. The observed variations indicate that local strains in the wavy ZnO microwire lead to strain-dependent local changes of its energy band structure. The local bending curvature calculations using a geometric model also provide correlation between the shift of the near-band-edge emission peaks and the bending strain.

(Some figures may appear in colour only in the online journal)

1. Introduction

Recently, strain engineering, which is a useful route to tune the band structure and physical properties of materials, has attracted considerable interest for nano/microstructures [1–6]. In particular, the strain effects of ZnO nano/microstructures have been intensively studied due to their tunable electronic and optical properties via strain engineering [3–13]. Because the strain induced by externally applied forces significantly affects the physical properties of ZnO, information about the strain distribution can play an important role in many potential applications, including stretchable and wearable applications that utilize the deformation of ZnO-based materials. Accordingly, for more technically challenging applications such as bio-integrated devices and bio-inspired designs, nano/microstructures must be able to deform into complex and curvilinear shapes, beyond simple bending [14]. To date, however, research efforts have focused on understanding the strain effects on the band structure and electronic and optical properties for simply bent ZnO nano/microstructures [3–13]. The curvilinear shapes that accommodate large deformation, including large tension, compression, bending, and twisting along the entire length of the ZnO nano/microstructure, could prove valuable for stretchable and wearable device applications. To our knowledge, the strain effects of ZnO nano/microstructures with complex and curvilinear shapes have not yet been studied.

In this study, strain-induced bandgap modulation is investigated using cathodoluminescence (CL) measurements, through the fabrication of a ZnO microwire with wavy configurations. The microwire was laterally buckled by applying and releasing external mechanical strains using elastomeric polydimethylsiloxane (PDMS) substrates, and transferred onto an epoxy-coated SiO_2 substrate. The variations in peak position and full width at half maximum (FWHM) of near-band-edge (NBE) emissions in CL spectra along the wavy ZnO microwire were measured at room temperature. Specifically, curved sections of the wavy ZnO microwire show red-/blue-shifts of the NBE and broadening of FWHM compared with straight sections. From these results, we find that for the wavy structure, the maximum local strains occur at localized positions (peaks and valleys), which

lead to the strain-induced modulation of the energy bandgap of the wavy ZnO microwire.

2. Experimental details

The ZnO microwires used in this study were grown using a vapor phase transport process, as described elsewhere [8, 15–17]. The structural and optical properties of the ZnO microwires were characterized using electron microscopy (scanning electron microscopy (SEM) and transmission electron microscopy (TEM)) and microphotoluminescence (μPL) spectroscopy. The μPL spectra were measured using a He–Cd laser (325 nm) as an excitation source at room temperature. For the formation of lateral buckling of the ZnO microwire, elastomeric substrates of PDMS (Sylgard 184, Dow Corning) were prepared by mixing a base resin and a curing agent with a ratio of 10:1. The air bubbles were then removed and the substrates were cured at 68 °C for 12 h in a vacuum oven. The PDMS slab, cut into a 40 mm × 10 mm slab, was uniaxially stretched by tens of per cent of strain and clamped by a custom-made strain stage through which the desired strain level could be achieved. A straight ZnO microwire was first placed on a prestrained PDMS substrate using a contact printing method [18], and then the ZnO microwire was laterally buckled by fully releasing the prestrain. In the transfer process, the microwire can be transferred onto the PDMS without damaging it. To avoid additional strain effects of the wavy ZnO microwire on the PDMS during the CL measurements, the wavy ZnO microwire was transferred onto a rigid SiO_2 (100 nm) substrate coated with an epoxy film (*SU*-8) at mild temperature (~70 °C). The epoxy film plays an important role in retaining the wavy shape after removal of the PDMS. To investigate the strain-induced influences on the energy bandgap of the wavy ZnO microwire, the NBE emission of the wavy ZnO microwire was measured at room temperature using CL spectroscopy (Gatan MonoCL3, electron beam energy of 9 kV).

3. Results and discussion

Figure 1(a) shows an SEM image of the beltlike ZnO microwire. A selected area electron diffraction (SAED) pattern (figure 1(b)) taken along the $[1\bar{1}00]$ zone axis, which is parallel to the vertical direction of its cross-section, indicates that the growth direction is $[1\bar{1}00]$ and the ZnO microwire is a single-crystalline structure. Note that the as-grown microwires can have different shapes and sizes because carbothermal reduction is a highly random growth process. No defects, such as dislocations or stacking faults, are found, indicating that the ZnO microwire is highly crystalline. This is also well supported by μPL spectra. Figure 1(c) shows μPL spectra measured at room temperature along the length of the as-grown ZnO microwire at each position from 1 to 6. The PL emissions of the ZnO microwire consist of two main bands. One is the NBE excitonic related emission band with a wavelength range between 375 and 420 nm. The other is the broad deep-level (DL)-related emission in the visible

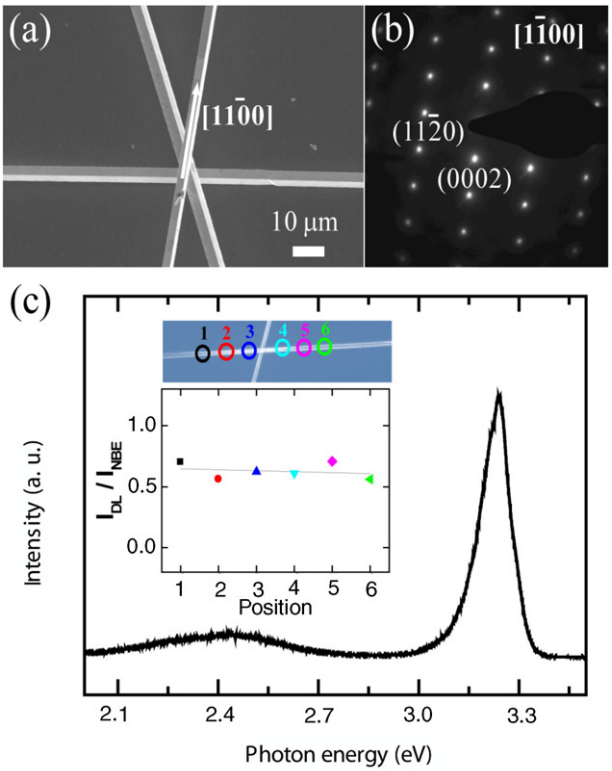

Figure 1. (a) An SEM image of as-grown ZnO microwires, and (b) their representative corresponding SAED pattern taken along the $[1\bar{1}00]$ zone axis. (c) A representative μPL spectrum of the single ZnO microwire at room temperature. The inset shows the integrated-PL intensity ratio (I_{DL}/I_{UV}) at each position. The colored circle-symbols in the inset (an optical image of the ZnO microwire) indicate the μPL measurement positions.

range that is attributed to the surface defects of the crystal. Thus, DL-related emission is determined by the concentration of the corresponding surface defects [12–14]. As shown in figure 1(c), the μPL spectra collected from the positions show much stronger NBE emission peaks than those of the DL-related emission peaks. The inset of figure 1(c) shows integrated-PL intensity ratios (DL-related emission intensity to NBE emission intensity, I_{DL}/I_{NBE}) obtained from the PL spectra at different positions from 1 to 6. The as-grown ZnO microwire exhibits small and uniform I_{DL}/I_{NBE} values at each position (the inset of figure 1(c)). These results provide experimental evidence that the ZnO microwire has a quite small density of surface defects because the DL-related emission peak is a surface-related process [19–21], indicating that the microwire is highly crystalline.

Figure 2 presents a schematic illustration of the fabrication and transfer processes of the ZnO microwire with wavy configurations onto an epoxy-coated SiO_2 substrate. The straight ZnO microwire was placed on a prestrained PDMS slab using a contact printing method [18], followed by release of the prestrain. Releasing the prestrain in the PDMS slab led to the formation of the wavy ZnO microwire on the plane of the PDMS surface due to compressive strains that cause the straight ZnO microwire to buckle laterally [22–24]. This indicates that the prestrain of the PDMS substrate in

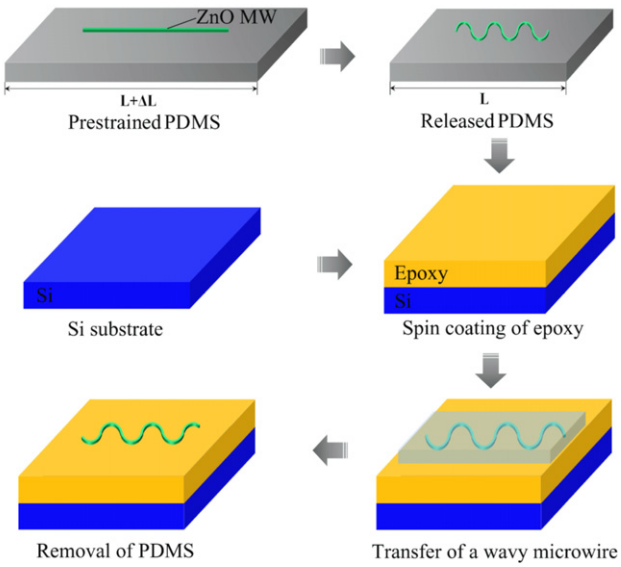

Figure 2. Schematic illustration of the formation and transfer processes onto an epoxy-coated SiO_2 substrate of a single ZnO microwire with wavy configurations.

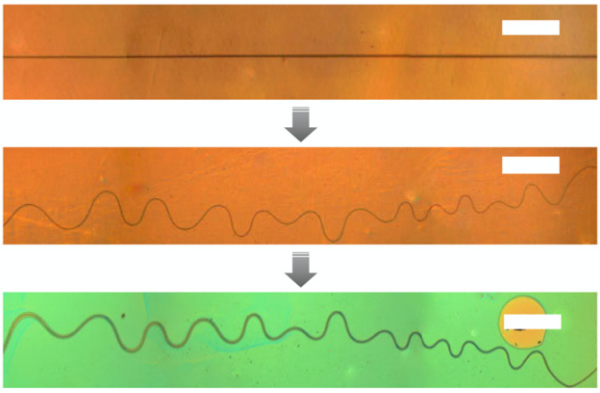

Figure 3. Optical images of a straight ZnO microwire on a prestrained PDMS slab (top), the laterally buckled ZnO microwire after releasing the prestrain of the PDMS slab (middle), and the wavy ZnO microwire transferred onto the SiO_2 substrate. The scale bars are 200 μm.

this process plays a critical role in the lateral buckling of the straight ZnO microwire. The wavy ZnO microwire formed in this manner was transferred onto an epoxy-coated SiO_2 substrate by conformal contact of the PDMS slab with the epoxy-coated substrate. Figure 3 shows optical images of a ZnO microwire on the prestrained PDMS (top), its lateral buckling on released PDMS (middle), and the laterally buckled ZnO microwire transferred onto the epoxy-coated SiO_2 substrate (bottom).

To investigate the strain-induced effects on the energy band and optical properties of the wavy ZnO microwire, we measured a series of NBE emissions of CL spectra in curved and straight sections of the wavy ZnO microwire. Figure 4(a) shows a representative SEM image of the wavy ZnO microwire on the epoxy-coated SiO_2 substrate.

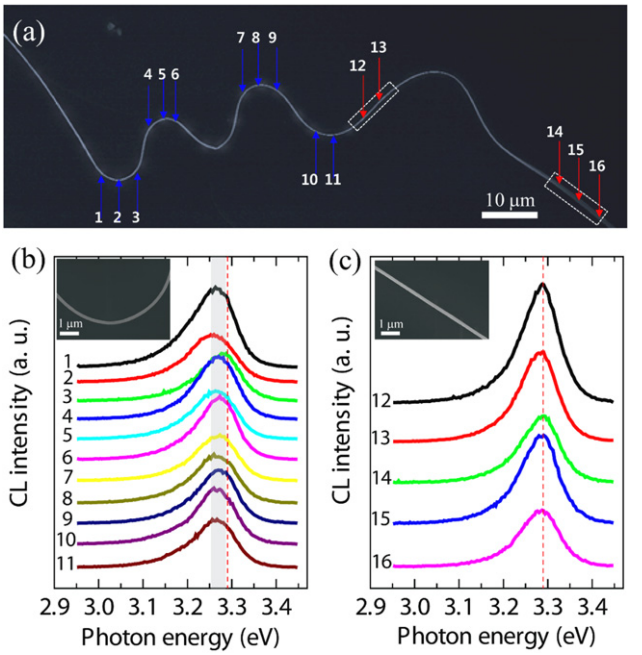

Figure 4. (a) An SEM image of a wavy ZnO microwire on an epoxy-coated SiO_2 substrate. (b), (c) CL spectra of the wavy ZnO microwire for, (b) curved sections (1–11, marked by blue arrows), and (c) straight sections (12–16, marked by red arrows). Each inset shows representative SEM images of the curved and straight sections in the wavy ZnO microwire. The red dashed line indicates the NBE emission of ∼3.29 eV in straight sections of the wavy ZnO microwire.

Figures 4(b) and (c) show CL spectra at curved sections (marked by blue arrows, 1–11) and straight sections (marked by red arrows, 12–16) respectively, along the wavy ZnO microwire. The CL spectra in curved sections (positions 1–11) of the wavy ZnO microwire exhibit shifts in the NBE emission peaks (marked by the gray color) and a broadening of the FWHM, whereas those in straight sections (positions 12–16) do not show any noticeable changes in the NBE emission peaks and their FWHM. We find that the NBE peaks move toward the lower energies in curved sections, indicating the bandgap modulation induced by localized strains.

From the CL spectra (figures 4(b) and (c)), we summarized the variations in the photon energy and the FWHM of NBE emission in curved and straight sections of the wavy ZnO microwire, as shown in figures 5(b) and (c). To understand the correlation between the shift of the NBE emission peaks and the bending strain, we considered local bending curvature calculations. According to Xue *et al* [25] and Dietrich *et al* [8], the maximum amount of tensile and compressive strain ε_{max} that is induced into the microwire by mechanical bending depends on the diameter of the microwire and the radius of curvature R, and it can be approximately calculated as $\varepsilon_{max.} = \pm d/2R$, where d is the diameter of the microwire ($d = 0.32$ μm). Based on the CL data and the strain–energy shift analysis using the geometric model [25], we approximately estimated the relationship between the shift of NBE emission energy and the variation of strain for the wavy ZnO microwire with various local bending curvatures.

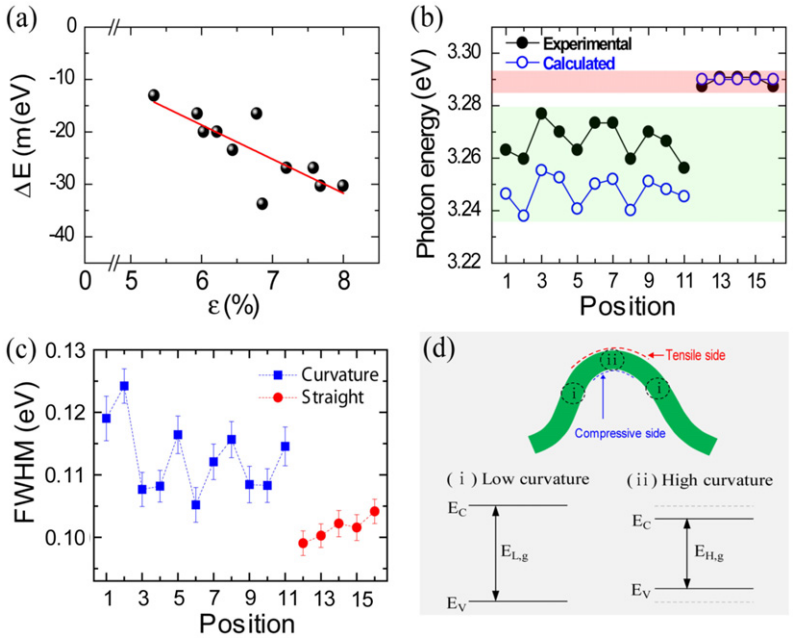

Figure 5. (a) The relationship between the shift of NBE emission energy and the variation of strain for the wavy ZnO microwire. (b) Calculated and experimental variations in NBE emission peaks in the CL spectra of curved sections (green color region) and straight sections (red color region) for the wavy ZnO microwire. (c) Variations in the FWHM of NBE emission peaks in the CL spectra in curved sections (figure 4(b)) and straight sections (figure 4(c)) of the wavy ZnO microwire. (d) A schematic illustration of strain-induced bandgap and band structure at sections with low and high curvatures in the wavy ZnO microwire. $E_{g,L}$ and $E_{g,H}$ indicate electronic energy gaps at sections with low and high curvatures, respectively.

In figure 5(a), the shift of NBE emission peaks can be fitted with a linear relation $\Delta E \propto \varepsilon$. Compared to the straight sections, for the wavy microwire, the photon energy of the NBE emission for the curved sections of the microwire shifts to a lower energy, indicating that the deformation induces inhomogeneous bandgap across the cross-section of the wavy microwire. This is consistent with experimental results (figures 5(b) and (c)) and previous reports [3, 25, 26].

In figure 5(b), the photon energies of NBE peaks in straight positions exhibit ~3.29 eV, whereas those in curved positions exhibit a lower energy range between ~3.26 and ~3.275 eV. The straight sections of the wavy ZnO microwire do not exhibit any noticeable change of the photon energy or FWHM of the NBE emission in the CL spectra. In contrast, for the curved sections (marked by green color, positions 1–11), the variations in the photon energy of the NBE emission and their FWHM show a tendency corresponding to a low–high–low curvature cycle (positions 1–3, 4–6, 7–9, and 10–11), as shown in figures 5(b) and (c). In addition, the broadening of the NBE peaks (figure 5(c)) can originate from the broadening of the gaps between sub-bands in the conduction band under strain-induced deformation [3]. Interestingly, we find that for the curved sections of the wavy microwire, sections with high curvature (i.e., peaks and valleys of in-plane waves (figure 4(a)), positions 2, 5, 8, and 11) exhibit relatively lower photon energies of NBE emission and larger FWHM values than those with low curvature (positions 1, 3, 4, 6, 7, 9 and 10). The blue/red shift tendency in the photon energy of the NBE emission corresponding to a low–high–low curvature cycle depends on the radius of the local bending curvatures, indicating the existence of localized inhomogeneous strains. This supports well the result of strain-induced reduction in the bandgap with the decrease of the radius of curvature. These results indicate that the lateral buckling deformation of the ZnO microwire induces the inhomogeneous strains (tensile and compressive strains) at the piezoelectric field, resulting in the modulation of the spatial distribution of photoexcited carriers in the curved sections. Consequently, the CL intensity from the outer surface (tensile side) of the microwire is much stronger than that from the inner surface (compressive side) of the microwire. This is in good agreement with previous results [3–8, 26]. It should be noted that the CL measurement cannot reflect fully the strain effect exactly at the focused point due to the scattering effect of the incident electron beam and the diffusion effect of excitons [3]. Such localized inhomogeneous strains lead to the local changes of the energy bandgap and the band structure in the wavy ZnO microwire because the conduction band energy (E_C) and the valence band energy (E_V) are sensitive to the axial strain and the surface in-plane strain under a localized strain state [6, 27, 28]. The increase of tensile strain with decreasing the radius of curvature results in overall strain-induced reduction in the energy bandgap. Therefore, sections of the wavy ZnO microwire with high curvature exhibit a relatively smaller energy bandgap ($E_{g,H}$) due to a higher strain state, whereas those with low curvature exhibit a larger energy bandgap ($E_{g,L}$) due to a lower strain state, as illustrated in figure 5(d).

4. Conclusions

In summary, we have investigated the strain-induced modulation of the bandgap in a ZnO microwire with wavy configurations using CL measurements. Curved sections of the wavy ZnO microwire show red-/blue-shifts and broadening of the FWHM in NBE peaks of the CL spectra along the length of the wavy ZnO microwire, indicating strain-induced modulation of bandgap. For the wavy ZnO microwire, the maximum local strains occur at localized positions (peaks and valleys of in-plane waves), which lead to overall strain-dependent reduction in the bandgap. This work will provide valuable information to design and develop ZnO-based devices for more challenging applications such as bio-integrated devices and bio-inspired designs via strain engineering.

Acknowledgments

WKH acknowledges the financial support from the Korea Basic Science Institute (KBSI) grant (T33516). JIS and SNC acknowledge the financial support from the Korea Institute of Energy Technology Evaluation and Planning (KETEP) (20128510010080). TL acknowledges the financial support from the National Creative Research Laboratory program (Grant No. 2012026372) of Korea.

References

[1] Chen J, Conache G, Pistol M-E, Gray S M, Borgström M T, Xu H, Xu H Q, Samuelson L and Håkanson U 2010 Probing strain in bent semiconductor nanowires with Raman spectroscopy *Nano Lett.* **10** 1280–6

[2] Cao J *et al* 2009 Strain engineering and one-dimensional organization of metal–insulator domains in single-crystal vanadium dioxide beams *Nature Nanotechnol.* **4** 732–7

[3] Han X *et al* 2009 Electronic and mechanical coupling in bent ZnO nanowires *Adv. Mater.* **21** 4937–41

[4] Han X, Kou L, Zhang Z, Zhang Z, Zhu X, Xu J, Liao Z, Guo W and Yu D 2012 Strain-gradient effect on energy bands in bent ZnO microwires *Adv. Mater.* **24** 4707–11

[5] Han X, Jing G, Zhang X, Ma R, Song X, Xu J, Liao Z, Wang N and Yu D 2009 Bending-induced conductance increase in individual semiconductor nanowire and nanobelts *Nano Res.* **2** 553–7

[6] Wei B, Zheng K, Ji Y, Zhang Y, Zhang Z and Han X 2012 Size-dependent bandgap modulation of ZnO nanowires by tensile strain *Nano Lett.* **12** 4595–9

[7] Liao Z-M *et al* 2012 Strain induced exciton fine-structure splitting and shift in bent ZnO *Sci. Rep.* **2** 452

[8] Dietrich C P, Lange M, Klüpfel F J, Wenckstern H v, Schmidt-Grund R and Grundman M 2011 Strain distribution in bent ZnO microwires *Appl. Phys. Lett.* **98** 031105

[9] Yan B, Chen R, Zhou W, Zhang J, Sun H, Gong H and Yu T 2010 Localized suppression of longitudinal–optical–phonon–exciton coupling in bent ZnO nanowires *Nanotechnology* **21** 445706

[10] Guo W, Yang Y, Liu J and Zhang Y 2010 Tuning of electronic transport characterization of ZnO micro/nanowire piezotronic Schottky diodes by bending: threshold voltage shift 2010 *Phys. Chem. Chem. Phys.* **12** 14868–72

[11] Gao Y and Wang Z L 2007 Elecctrostatic potential in a bent piezoelectric nanowire. The fundamental theory of nanogenerator and nanopiezotronics *Nano Lett.* **7** 2499–505

[12] Wang Z L 2007 Nanopiezotronics *Adv. Mater.* **19** 889–92

[13] Wang X, Song J, Liu J and Wang Z L 2007 Direct-current nanogenerator driven by ultrasonic waves *Science* **316** 102–5

[14] Rogers J A, Someya T and Huang Y 2010 Materials and mechanics for stretchable electronics *Science* **327** 1603–7

[15] Hong W-K *et al* 2008 Tunable electronic transport characteristics of surface-architecture-controlled ZnO nanowire field effect transistors *Nano Lett.* **8** 950–6

[16] Pan Z W, Dai Z R and Wang Z L 2001 Nanobelts of semiconducting oxides *Science* **291** 1947–9

[17] Hu Y, Chang Y, Fei P, Snyder R L and Wang Z L 2010 Desinging the electric transport characteristics of ZnO micro/nanowire devices by coupling piezoelectric and photoexcitation effects *ACS Nano* **4** 1231–40

[18] Fan Z, Ho J C, Jacobson Z A, Yerushalmi R, Alley R L, Razavi H and Javey A 2008 Wafer-scale assembly of highly ordered semiconductor nanowire arrays by contact printing *Nano Lett.* **8** 20–5

[19] Shalish I, Temkin H and Narayanamurti V 2004 Size-dependent surface luminescence in ZnO nanowires *Phys. Rev.* B **69** 245401

[20] Djurišić A B, Choy W C H, Roy V A L, Leung Y H, Kwong C Y, Cheah K W, Rao T K G, Chan W K, Lui H F and Surya C 2004 Photoluminescence and electron paramagnetic resonance of ZnO tetrapod structure *Adv. Funct. Mater.* **14** 856–64

[21] Zhou X, Kuang Q, Jiang Z-Y, Xie Z-X, Xu T, Huang R-B and Zheng L-S 2007 The origin of green emission of ZnO microcrystallites: surface-dependent light emission studied by cathodoluminescence *J. Phys. Chem.* C **111** 12091–3

[22] Ryu S Y, Xiao J, Park W I, Son K S, Huang Y Y, Paik U and Rogers J A 2009 Lateral buckling mechanics in silicon nanowires on elastomeric substrates *Nano Lett.* **9** 3214–9

[23] Feng X, Yang B D, Liu Y, Wang Y, Dagdeviren C, Liu Z, Carlson A, Li J, Huang Y and Rogers J A 2011 Stretchable ferroelectric nanoribbons with wavy configurations on elastomeric substrates *ACS Nano* **5** 3326–32

[24] Xu F, Lu W and Zhu Y 2011 Controlled 3D buckling of silicon nanowires for stretchable electronics *ACS Nano* **5** 672–8

[25] Xue H, Pan N, Li M, Wu Y, Wang X and Hou J G 2010 Probing the strain effect on near band edge emission of a curved ZnO nanowire via spatially resolved cathodoluminescence *Nanotechnology* **21** 215701

[26] Xu S, Guo W, Du S, Loy M M T and Wang N 2012 Piezotronic effects on the optical properties of ZnO nanowires *Nano Lett.* **12** 5802

[27] Kou L, Li C, Zhang Z-Y, Chen C and Guo W 2010 Charge carrier separation induced by intrinsic surface strain in pristine ZnO nanowires *Appl. Phys. Lett.* **97** 053104

[28] Li Y F *et al* 2008 Biaxial stress-dependent optical band gap, crystalline, and electronic structure in wurtzite ZnO: experimental and *ab initio* study *J. Appl. Phys.* **104** 083516